EXPERIMENTAL STUDY ON DETERMINING THE TORSIONAL STIFFNESS OF ANTI-ROLL BAR IN TRUCK

Ngo Van Dung[1,2], Vu Van Tan[2,*], Truong Manh Hung[3]

DOI: http://doi.org/ 10.57001/huih5804.2025.261

ABSTRACT

This study focuses on developing a methodology to measure and determine the torsional stiffness of an anti-roll bar through experimental testing. A dedicated test system was constructed to simulate the actual loading conditions experienced at the end of the anti-roll bar during real-world vehicle operation. The testing procedure involved gradually applying load to one end of the bar while monitoring displacement at specific positions along the bar and recording force responses using high-precision sensors and the Dewesoft data acquisition system. The experimental data were then used to calculate torsional stiffness and compared with theoretical values derived from analytical formulas based on SAE standards. The geometric parameters and material properties of the anti-roll bar were incorporated into the model to ensure accuracy. The test results confirmed that the torsional stiffness of the anti-roll bar installed on the 15-ton ISUZU truck is 56420.24Nm/rad, providing a solid foundation for further mechanical analysis and design calibration of anti-roll bars for trucks. This research supports the improvement of suspension system design, contributing to enhanced safety, load control, and roll stability for large commercial vehicles.

Keywords: *Passive anti-roll bar, torsional stiffness, heavy-duty vehicle, Roll stability, Road safety.*

[1]Faculty of Automotive Engineering Technology, Thanh Do University, Vietnam
[2]Faculty of Mechanical Engineering, University of Transport and Communications, Vietnam
[3]Motor Vehicle Technical Safety Inspection Dept (VAR), Vietnam Register (VR), VietNam
[*]Email: vvtan@utc.edu.vn
Received: 01/6/2025
Revised: 10/7/2025
Accepted: 25/7/2025

1. INTRODUCTION

The anti-roll bar, also known as the stabilizer bar, plays a critical role in enhancing the roll stability of vehicles by reducing body roll during cornering and ensuring balanced load transfer between wheels [1]. In heavy-duty trucks, particularly those with dependent suspension systems like the ISUZU 15-ton vehicle, the anti-roll bar becomes even more vital due to the high center of gravity and large axle loads. The performance of this component directly influences road-holding capability, steering behavior, vehicle comfort and its stabilyties [2, 3].

Key parameters determining the effectiveness of the anti-roll bar include its geometric configuration - such as the arm length, outer diameter, and mounting distances - and its material properties, notably the modulus of elasticity and moment of inertia [4]. These parameters together define the torsional stiffness, which quantifies the bar's resistance to twisting under load. Accurate determination of torsional stiffness is essential for suspension tuning and vehicle dynamics optimization [5, 6].

The torsional stiffness of anti-roll bars has long been a subject of interest in vehicle dynamics research due to its direct impact on roll stability and ride comfort. Numerous methods have been developed to estimate or measure this property. At the conceptual design stage, analytical approaches based on classical beam theory and Castigliano's theorem are frequently employed [7]. These methods provide quick estimations by relating torque and angular displacement using geometric and material properties of the anti-roll bar. While these formulas are useful for preliminary analysis, they often assume idealized boundary conditions and simplified geometry, limiting their accuracy in complex vehicle configurations [8].

Numerous studies have investigated the design and control of anti-roll bar systems to enhance vehicle roll stability and comfort. For instance, Pi Dawei et al. [9] proposed a hydraulic active stabilizer bar system integrated with a feedforward and fuzzy-PID control strategy. Their work demonstrated that active control of

stabilizer torque could significantly reduce vehicle roll and improve yaw stability during cornering. In another study, Varga et al. [10] presented a hierarchical control approach for anti-roll bar systems, optimizing ride comfort and handling by coordinating multiple control layers. Similarly, hardware-in-the-loop (HIL) testing frameworks have been used to validate robust roll control algorithms, as shown by experimental setups that simulate real-time vehicle dynamics and actuator responses [11]. While these studies focus primarily on active control and real-time implementation, the experimental determination of torsional stiffness remains essential for validating physical models and tuning controller parameters [12]. Compared to control-focused works, the present study contributes by establishing an experimental test system specifically for measuring the torsional stiffness of an anti-roll bar used in a 15-ton ISUZU truck. This provides a foundational mechanical dataset that supports both passive and active suspension system design and ensures model fidelity in simulation and control development. The key contribution of this paper lies in establishing a repeatable and accurate experimental procedure to assess anti-roll bar stiffness in heavy-duty vehicles. The findings provide a reliable basis for evaluating suspension performance, enabling model calibration, component tuning, and the enhancement of vehicle stability and load-handling performance in commercial transport applications.

This article structure as follows: Section 2 deploys the torsional stiffness of the anti-roll bar according to SAE; Section 3 developing experimental procedure to determine the torsion stiffness of horizontal stabilizer bars; Section 4 experimental results for determining the torsional stiffness of the anti-roll bar; Section 5 is the conlusions.

2. TORSIONAL STIFFNESS OF THE ANTI-ROLL BAR ACCORDING TO SAE

The design of an anti-roll bar essentially involves creating a component that achieves the required torsional stiffness. This enhances the vehicle's roll stability without exceeding the mechanical limitations of the anti-roll bar material. SAE has provided formulas for calculating the torque and force acting on the anti-roll bar in the *"Spring Design Manual"* [8]. Several formulas are used to determine the stiffness of the anti-roll bar and the deflection at the bar's end under a given force. The standard geometric dimensions of the anti-roll bar are illustrated in Fig. 1. A load F is applied at point A, directed either inward or outward from the plane of the page. The stiffness of the bar can be calculated using the SAE formula [8] as follows:

$$c_{af} = \frac{FL^2}{2f_A}\left(\frac{Nm}{rad}\right) \quad (1)$$

where f_A is the displacement at point A under the action of force F; L is half the length of the anti-roll bar. The displacement f_A is determined using equation (2).

$$f_A = \frac{F}{3EI}\chi \quad (2)$$

in which $I = \frac{\pi D^4}{64}$ is the moment of inertia of the bar; *D* is the outer diameter of the bar; E is the Young modulus; χ is the correction factor accounting for structural parameters affecting the torsional stiffness of the anti-roll bar, $\chi = f(a,b,c_1,c_2,e,f,l_1,l_2,l_3,L,L')$.

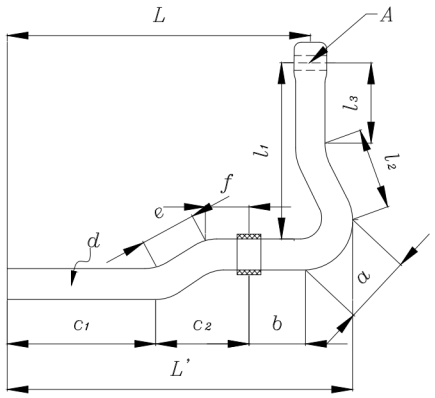

Fig. 1. Half anti-roll bar shape and its dimensions [8]

The torsional stiffness of the anti-roll bar can also be determined using the following formula:

$$c_{af} = \frac{3EIL^2}{2\chi}\left(\frac{Nm}{rad}\right) \quad (3)$$

For the suspension system of the ISUZU 15-ton truck used in the experimental model, the vehicle features a dependent suspension system, in which a rigid axle connects the two wheels on the same axle. The geometric parameters of the anti-roll bar are presented in Table 1.

Table 1. Table of geometric parameters of the anti-roll bar for the ISUZU 15-ton truck

Symbol	Value	Unit	Symbol	Value	Unit
l_1	430	mm	c_1	430	mm
l_2	160	mm	f	60	mm
l_3	150	mm	e	100	mm
a	90	mm	L	510	mm

b	140	mm	L'	565	mm
c_2	150	mm			

The torsional stiffness of the anti-roll bar during the experimental process is calculated using equation (4):

$$c_{af} = \frac{PgL^2}{2f_A}\left(\frac{Nm}{rad}\right) \quad (4)$$

in which, P is the load applied at the end of the anti-roll bar (kg), and g is the gravitational acceleration.

3. DEVELOPING EXPERIMENTAL PROCEDURE TO DETERMINE THE TORSION STIFFNESS OF ANTI-ROLL BARS

3.1. Experimental test bench design

Fig. 2 presents the experimental setup diagram used to determine the torsional stiffness of the anti-roll bar installed on a truck. This is a specialized mechanical measurement and testing system designed to simulate the actual working conditions of the anti-roll bar when the vehicle is subjected to torsional moments during operation, particularly when cornering or when there is an uneven load distribution between the two sides of the vehicle.

The basic components of the system include:

(1) A support plane for the anti-roll bar bearings, serving as the main structure to fix and position both ends of the anti-roll bar throughout the experiment.

(2) The anti-roll bar is installed into the system through these bearings, ensuring the bar's structure remains stable under conditions where no displacement occurs at the fixed points.

(3) At the midpoint of the anti-roll bar, the bar is supported to prevent unwanted vertical movement while maintaining the geometric stability of the entire structure.

One end of the anti-roll bar, labeled as (4), is where mechanical input from the actuator system is applied. Specifically, at (5) the end of the anti-roll bar in contact with the lifting jack, force is transmitted to the bar through a precisely placed contact point to generate a torsional moment that accurately reflects the bar's real-world operating conditions. To produce this force, the system uses (7) a hydraulic lifting jack, which allows precise adjustment of the force magnitude according to experimental requirements.

The anti-roll bar lever arm (6) acts as an intermediate component, transmitting force from the lifting jack to the anti-roll bar while creating the necessary lever arm to effectively generate torsional moment. The force at the contact point is directly measured by (8) a force sensor, enabling high-precision recording of applied force parameters for calculating torsional stiffness using mechanical analysis methods.

Data from the force sensor and other related sensors are transmitted to (9) the Dewesoft data measurement and analysis device, a specialized signal acquisition and processing system capable of providing real-time measurement results. This device allows for data synchronization, storage, and analysis of torsional moment, twist angle deviation, and other influencing factors, thereby supporting the accurate determination of the anti-roll bar's torsional stiffness.

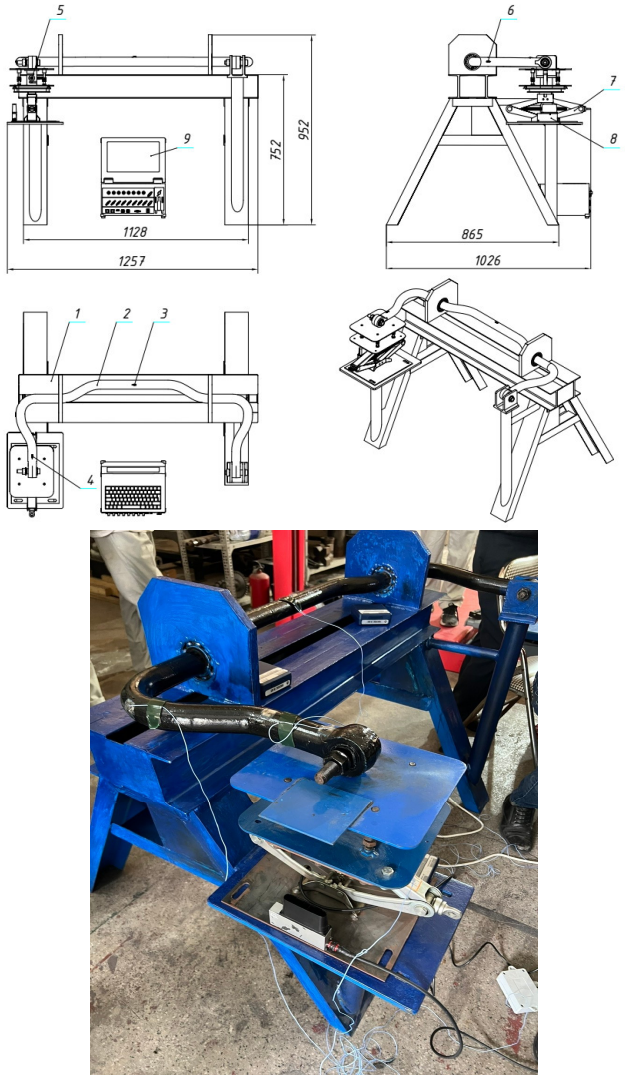

Fig. 2. The test rig, sensors, and specialized data acquisition computer system were all designed using Autodesk Inventor 2023

According to the design specifications, the test rig is constructed in the shape of an "A" frame, with maximum

dimensions of 1257mm in length, 1026mm in width, and 952mm in height. To enhance structural rigidity and ensure stability during the experimental process, the entire frame is fabricated using I-beam steel sections. The setup includes a rigid clamping mechanism mounted on one arm of the A-frame to securely fix one end of the anti-roll bar. On the opposite side, a specially designed support base is integrated with a hydraulic jack, which is used to apply controlled force to the free end of the anti-roll bar. In addition, the two rubber bushings located at the midpoint of the anti-roll bar are supported by fixed-position mounts that only allow rotational movement of the bar around the axis defined by the bushings. This configuration ensures realistic simulation of the anti-roll bar's operational constraints in a vehicle while maintaining measurement accuracy during the torsional stiffness evaluation.

3.2. Experimental equipment

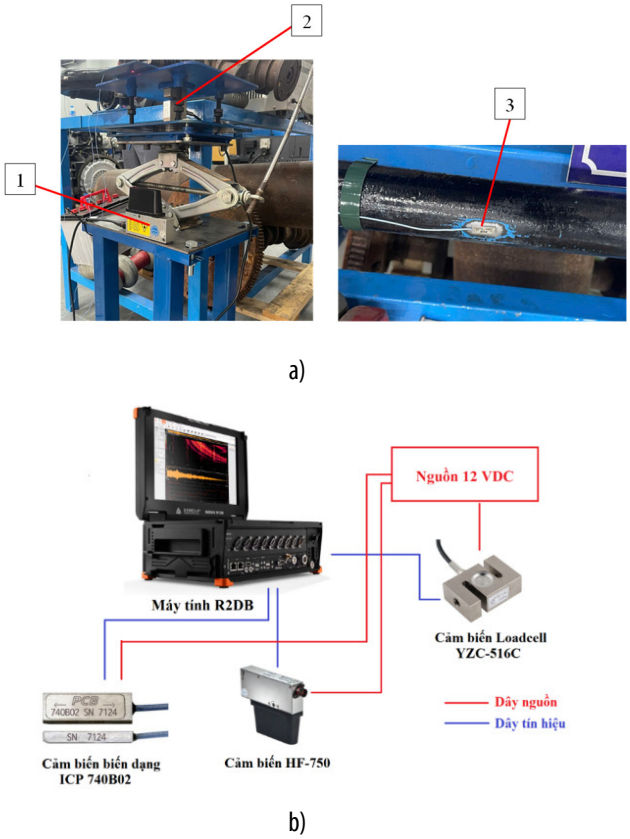

Fig. 3. Diagram of experimental equipment connection to the model: (1) HF-750 displacement sensor; (2) 516C load cell sensor; (3) ICP 740B02 strain sensor

The experimental system designed to determine the torsional stiffness of the anti-roll bar in a commercial truck is equipped with a comprehensive set of modern sensors and measurement devices to ensure high accuracy in data acquisition and processing. Specifically, three primary types of sensors are employed in the setup: the HF-750 displacement sensor (position 1 in figure 3a), the YZC-516C load cell sensor (position 2 in Fig. 3a), and the ICP 740B02 strain gauge sensor (position 3 in Fig. 3a). These sensors are strategically placed on the model to accurately capture the force input, displacement, and stress responses at key points along the anti-roll bar.

The schematic diagram of the equipment connections, shown in Fig. 3b, illustrates that all sensors are directly connected to the Dewesoft R2DB data acquisition and signal analysis system. The YZC-516C load cell is powered by a 12VDC supply and transmits measurement signals to the analysis unit via signal cables. Similarly, the HF-750 displacement sensor and the ICP 740B02 strain gauge are connected through their respective signal lines. All sensor signals are synchronously collected and processed in real time using the Dewesoft software platform, which enables precise visualization, storage, and analysis of the experimental data.

Table 2. Technical Specifications of Loadcell YZC-516C

Category	Specification	Value / Unit
Physical Dimensions	Mounting thread size	M12 x 1.75mm
	Signal cable size	Ø5.7mm, 3.5m long
	Length	51mm
	Width	19mm
	Height	76mm
	Weight	190mg
	Material	Alloy steel
Electrical Properties	Signal wire color coding	Red (E+), Black (E–), Blue (S+), White (S–)
	Excitation voltage	5 ~ 12VDC
	Input resistance	350 ± 5Ω
	Output resistance	350 ± 3Ω
	Insulation resistance	≥ 5000MΩ @ 100VDC
	Rated output	2.0 ± 0.005mV/V
Measurement Performance	Measuring range	0 ÷ 500kg
	Safe overload	150% FS
	Ultimate overload	200% FS
	Hysteresis	±0.03% FS
	Repeatability	±0.03% FS
	Creep (30 min)	±0.024% FS

Table 3. Technical Specifications of ICP Strain Sensor (Model ICP 740B02) [13]

Category	Specification	Value / Unit
Electrical Properties	Supply voltage	18 ÷ 30 V
	Output voltage	8 ÷ 14 V
Frequency Characteristics	Frequency range	0.5 ÷ 100,000 Hz
Sensitivity & Range	Sensitivity	50 mV/με
	Measurement range	100 pkμε
	Overload limit	±10,000 gpk
Environmental Conditions	Operating temperature range	−53 ÷ 121 °C

Table 4. Technical Specifications of Displacement Sensor HF-750 [14]

Category	Specification	Value / Unit
Measurement Range	Measuring range	750mm
Accuracy	Linearity	±0.2 ÷ ±0.3 %
Sampling Characteristics	Sampling rate	0.3 - 8kHz
Output Signal	Output signal	0 - 10V
Communication Interface	Connection ports	Analog, CAN, RS-232

3.3. Experimental Procedure

The experimental investigation was carried out in accordance with a well-defined protocol to ensure repeatability, safety, and the integrity of the acquired data. Prior to the commencement of testing, a preparatory session was conducted to provide comprehensive guidance on the technical steps required for the measurement process. All participating personnel were instructed on the proper handling and operation of the experimental equipment, with strict emphasis on compliance with the prescribed sequence of actions and safety procedures.

Following the preparation phase, the experiment was initiated by sequentially activating the components of the measurement system. The hydraulic actuation system - responsible for generating the external loading force - was powered on first to allow sufficient time for system stabilization. Only after confirming the stable operation of the hydraulic unit was the data acquisition system, including the connected computer and sensors, powered on. This startup sequence was deliberately implemented to ensure the synchronized and stable interaction between the mechanical and digital subsystems of the test environment.

Once the entire system was operational, configuration of the data acquisition and analysis software (Dewesoft) was undertaken. Within the software interface, appropriate measurement modes were selected based on the nature of the experiment. Real-time data acquisition parameters were set, including sampling frequency, signal filtering options, and data storage formats. In addition, metadata attributes for each test - such as sample identification, date, and sensor calibration values - were assigned to ensure traceability and reproducibility of the collected datasets.

The core of the experiment involved the gradual application of force through the hydraulic jack to simulate torsional loading conditions on the anti-roll bar. During this phase, the data recording function was activated to capture synchronized readings from multiple sensors, including load cells, displacement sensors, and strain gauges. The force increased incrementally while continuously monitoring the system response via the Dewesoft interface. Care was taken to ensure that the applied load reached a predefined target value and was maintained at a steady state for a sufficient duration to allow accurate measurement of the system's static response.

Upon achieving the target load and ensuring that all sensor outputs had stabilized, the hydraulic actuation was halted, and the data acquisition system automatically stored the experimental results in the predefined directory. Once data collection was complete, instructions were given to release the applied load and return the hydraulic jack to its initial position, either in preparation for a subsequent trial or to conclude the current test session. Following the conclusion of the experimental run, a structured shutdown procedure was executed. All active software applications were closed systematically to prevent data corruption. The computer and associated electronic devices were powered off, followed by the hydraulic system. Finally, all sensors, connectors, and mounting components were carefully disassembled and stored in their designated locations. This end-of-test protocol was implemented to protect the integrity of the equipment and to prepare the system for future testing.

4. EXPERIMENTAL RESULTS FOR DETERMINING THE TORSIONAL STIFFNESS OF THE ANTI-ROLL BAR

4.1. Loading Conditions for Determining the Torsional Stiffness of the Anti-Roll Bar

In order to enhance the precision and reliability of the experimental evaluation, multiple test trials were systematically conducted by varying the magnitude of

the maximum load applied to the end of the anti-roll bar. This approach allowed for a more comprehensive assessment of the mechanical behavior of the component under different loading conditions, while also minimizing the influence of random errors or environmental disturbances associated with individual measurements. Each trial was carried out under controlled conditions, and the results were carefully recorded and analyzed. The complete set of test data, including the corresponding maximum applied loads for each trial, is presented in Table 5, serving as the basis for subsequent analysis of the torsional stiffness characteristics of the anti-roll bar.

Table 5. Maximum applied load to anti roll bar

Test no.	Maximum applied load P at point A (kg)	Test duration (s)
1	150	29.40
2	200	31.68
3	250	38.20

During the testing process, the load is applied at point A of the anti-roll bar and is gradually increased over time until it reaches its maximum value, as presented in Table 5. Specifically, the load increases linearly over the first 15 seconds, rising from 0 to its peak value. After reaching this maximum load, the system maintains a constant load for at least 10 seconds to ensure stable operating conditions and to accurately assess the response of the anti-roll bar under high-load conditions. The loading process can be described by a time-dependent linear function as follows:

$$F(t)=\begin{cases}\frac{F_{max}}{15}t, & 0\le t<15(s)\\ F_{max}, & t\ge 15(s)\end{cases} \quad (5)$$

where F(t) is the applied force at time t; F_{max} is the maximum prescribed force as in Table 5.

4.2. Butterworth filter

To ensure the stability and reliability of the analysis results, a Butterworth filter - a widely used digital signal processing technique - was selected for the purpose of noise suppression and signal smoothing [15]. The Butterworth filter is characterized by a smooth and stable frequency response, exhibiting no ripples in either the passband or the stopband. This makes it particularly well-suited for applications that require the preservation of the signal's waveform post-filtering without distorting its original characteristics. The amplitude response of the Butterworth filter is defined by the following expression:

$$|H(j\omega)|=\frac{1}{\sqrt{1+\left(\frac{\omega}{\omega_c}\right)^{2n}}} \quad (6)$$

where, H(jω) represents the transfer function of the filter; ω is the angular frequency; ω_c is the cutoff frequency, and n denotes the order of the filter.

As the order n increases, the roll-off near the cutoff frequency ω_c becomes steeper, allowing for more effective noise suppression. However, this may also lead to a slower system response. Therefore, careful consideration is given to the selection of the filter order and cutoff frequency, aiming to preserve the essential physical characteristics of the output signal while minimizing the presence of undesired noise. Additionally, to implement the Butterworth filter in a digital environment, the analog transfer function must be transformed into the z domain using techniques such as the bilinear transformation. The general form of the resulting digital filter is expressed as:

$$H(z)=\frac{b_0+b_1z^{-1}+\cdots+b_nz^{-n}}{1+a_1z^{-1}+\cdots+a_nz^{-n}} \quad (7)$$

in which the coefficients a_i and b_i are computed from the specifications of the analog filter through a digitization design process.

4.3. Experiment results

To quantitatively evaluate the torsional stiffness of the anti-roll bar under controlled loading conditions, the analysis focused on the stable phase of the test in which the applied load reached its maximum and remained constant. Specifically, the average torsional stiffness was computed over the time interval beginning at 15 seconds - when the load stabilized - until the end of the experiment. The corresponding results are summarized in Table 5. The post-processed data, which had been filtered using a Butterworth digital filter to suppress high-frequency noise, were used to calculate the average torsional stiffness. This was accomplished using the *mean* function in MATLAB, based on the following numerical expression:

$$c_{af}=\text{mean}(c_{af\text{-}Butterworth}(t_{15s}:t_{end})) \quad (8)$$

in which $c_{af\text{-}Butterworth}$ denotes the average torsional stiffness by using Butterworth filter, t_{15s} is the sample index corresponding to 15 seconds; t_{end} is the final sample index of the test. This approach ensures both computational efficiency and statistical reliability in

estimating the mechanical response of the anti-roll bar during quasi-static conditions.

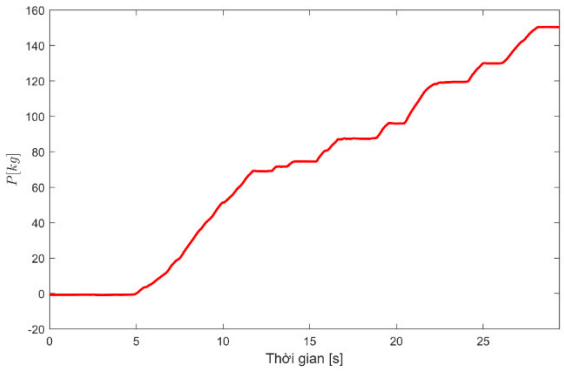

Fig. 4. The load applied to the end of the anti-roll bar during test 1

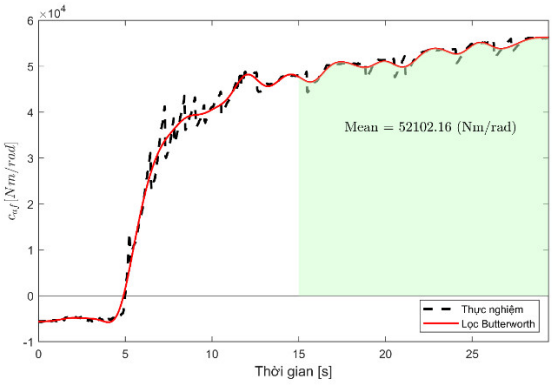

Fig. 5. The torsional stiffness of the anti-roll bar in test 1

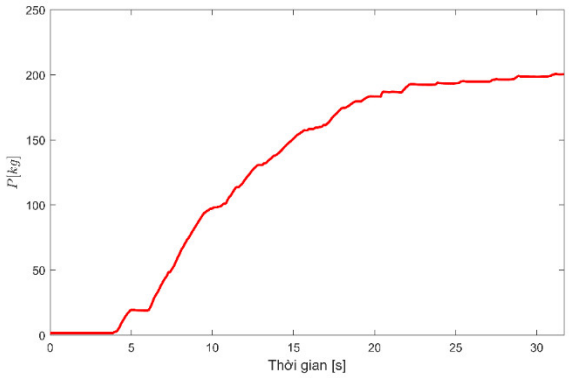

Fig. 6. The load applied to the end of the anti-roll bar during test 2

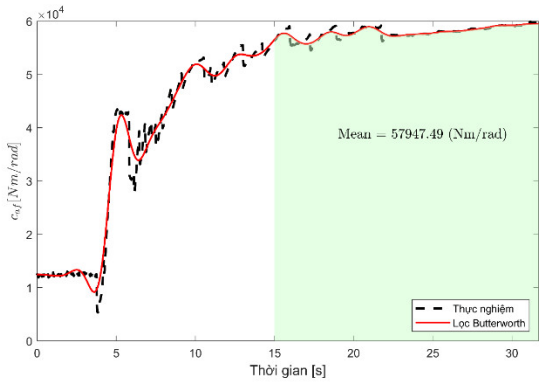

Fig. 7. The torsional stiffness of the anti-roll bar in test 2

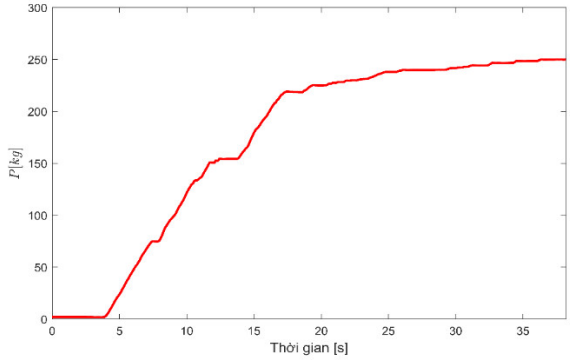

Fig. 8. The load applied to the end of the anti-roll bar during test 3

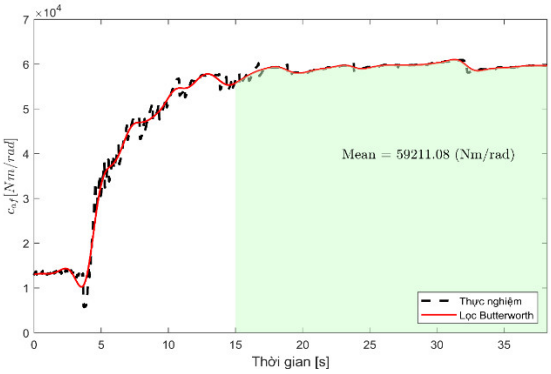

Fig. 9. The torsional stiffness of the anti-roll bar in test 3

Experimental findings illustrated in Figs. 5, 7, and 9 indicate that despite variations in the magnitude of the applied load P across different test iterations, the resulting torsional stiffness values remained relatively consistent. These small variations are attributed primarily to instrumentation noise and environmental disturbances rather than intrinsic variability in the structural characteristics of the anti-roll bar. Consequently, the average value of torsional stiffness obtained from multiple test runs is considered a robust indicator of the anti-roll bar's mechanical performance under the given loading scenario.

Table 6. The average torsional stiffness value of the anti-roll bar across each test iteration

Test no.	Average torsional stiffness $c_{af(i)}$
1	52102.16Nm/rad
2	57947.49Nm/rad
3	59211.08Nm/rad

From Table 6, in order to provide a comprehensive evaluation of the torsional stiffness of the anti-roll bar across multiple test iterations, the arithmetic mean of the measured values was employed. This approach effectively minimizes the influence of random errors and external disturbances that may occur in individual test runs, thereby offering a statistically reliable

representation of the mechanical characteristics of the anti-roll bar. The arithmetic mean is calculated using the following equation:

$$\overline{c}_{af} = \frac{1}{n}\sum_{i=1}^{n} c_{af(i)} \quad (9)$$

After three tests, the torsional stiffness value of the anti-roll bar, as measured using device (9), is c_{af} = 56420.24Nm/rad.

5. CONCLUSIONS

This research presents the design and experimental validation of a test system used to determine the torsional stiffness of the anti-roll bar installed on a 15-ton ISUZU truck. The test rig, developed using Autodesk Inventor 2023 and equipped with a Dewesoft data acquisition system, simulates real-world torsional loads experienced by the anti-roll bar during vehicle operation. A controlled loading process was applied linearly over time, and the corresponding angular deflection was measured with theoretical values calculated based on SAE guidelines, taking into account the bar's geometry, material properties, and boundary conditions. From three repeated tests, the average torsional stiffness was determined to be approximately 56420.24 Nm/rad, indicating good consistency and reliability of the experimental setup. The study provides a practical foundation for evaluating and improving suspension components in heavy-duty vehicles. The developed system can be used for future design optimization, model calibration, or durability testing under different loading scenarios. This research contributes valuable insight into the performance evaluation of vehicle anti-roll bars and supports further development in enhancing roll stability and load balancing in commercial vehicles.

ACKNOWLEDGEMENT

The author would like to express sincere thanks to colleagues at the Faculty of Mechanical Engineering, Thanh Do University; the lecturers of the Department of Automotive Mechanical Engineering, Faculty of Mechanical Engineering, University of Transport and Communications; and the Vietnam Register for their support during the course of this research.

REFERENCES

[1]. M. Cerit, E. Nart, K. Genel, "Investigation into effect of rubber bushing on stress distribution and fatigue behaviour of anti-roll bar," *Engineering Failure Analysis*, 17, 5, 1019-1027, 2010. doi: 10.1016/j.engfailanal.2010.01.009.

[2]. V. T. Vu, O. Sename, L. Dugard, P. Gaspar, "Enhancing roll stability of heavy vehicle by LQR active anti-roll bar control using electronic servo-valve hydraulic actuators," *Vehicle System Dynamics*, 55, 9, 1405-1429, 2017. doi: 10.1080/00423114.2017.1317822.

[3]. V. Van Tan, O. Sename, P. Gaspar, T. T. Do, *Active Anti-Roll Bar Control Design for Heavy Vehicles*. Springer Nature Singapore, 2024. doi: 10.1007/978-981-97-1359-2.

[4]. P. Tat Thang, T. Manh Quan, D. Trong Tu, N. Van Dung, V. Van Tan, "Evaluation of The Influence of Structural Parameters on the Characteristics of Anti-Roll Bars in Trucks by Using Finite Element Method," *Journal of Applied Engineering Science*, 1–10, 2025. doi: 10.5937/jaes0-55194.

[5]. P. Bharane, K. Tanpure, A. Patil, G. Kerkal, "Design, Analysis and Optimization of Anti-Roll Bar," *Int. Journal of Engineering Research and Applications,* 4, 9, 137-140, 2014.

[6]. Karan K. Sharma, Arshad Rashid, Saiprasad Mandale, "Analysis of Anti-Roll bar to Optimize the Stiffness," *International Journal of Modern Trends in Engineeringand Research*, 2, 7, 2015.

[7]. David Cebon, *Active Roll Control of Articulated Vehicles*. Ph.D Thesis, Cambridge University, 2000. doi: 10.1080/00423119608969300.

[8]. Society of Automotive Engineering, *Spring Design Manual.* 1996.

[9]. P. Dawei, K. Zhenxing, W. Xianhui, W. Hongliang, C. Shan, "Design and experimental validation of control algorithm for vehicle hydraulic active stabilizer bar system," in *Proceedings of the Institution of Mechanical Engineers, Part D: Journal of Automobile Engineering*, 233, 5, 1280–1295, 2019. doi: 10.1177/0954407018770539.

[10]. B. Varga, B. Németh, P. Gáspár, "Design of Anti-Roll Bar Systems Based on Hierarchical Control," *Strojniški vestnik - Journal of Mechanical Engineering*, 61, 6, 374-382, 2015. doi: 10.5545/sv-jme.2014.2224.

[11]. H.J. Kim, H. S. Yang, Y.P. Park, "Robust roll control of a vehicle: Experimental study using a hardware-in-the-loop set-up," in *Proceedings of the Institution of Mechanical Engineers, Part D: Journal of Automobile Engineering*, 216, 1, 1-9, 2002. doi: 10.1243/0954407021528850.

[12]. D.W. Pi, N. Chen, B. J. Zhang, "Experimental demonstration of a vehicle stability control system in a split-μ manoeuvre," in *Proceedings of the Institution of Mechanical Engineers, Part D: Journal of Automobile Engineering*, 225, 3, 305-317, 2011. doi: 10.1177/09544070JAUT01541.

[13]. PCB Piezoelectronics, *Piezoelectric Strain Sensor*. [Online]. Available: https://www.pcb.com/products?m=740b02

[14]. Kistler, *HF sensors/CHFA.* [Online]. Available: https://www.kistler.com/INT/en/cp/optical-laser-height-sensors-chfa/P0000846

[15]. M. T. Thompson, "Analog Low-Pass Filters," in *Intuitive Analog Circuit Design*, 531-583, 2014. doi: 10.1016/B978-0-12-405866-8.00014-0.